CALICE Analysis Note CAN-032
March 25, 2011

DHCAL Response to Positrons and Pions

The CALICE Collaboration[1]

Abstract

This note reports on the preliminary results of beam tests with the large CALICE DHCAL prototype. The prototype was tested in October 2010 and January 2011 at FNAL. Within the full analyses program, a prompt methodology was developed to access the calorimetric properties. Here we report on the application of this methodology to the October 2010 beam test data.

1 Corresponding author: Burak Bilki; burak-bilki@uiowa.edu

Contents

1. Introduction 3

2. Analysis Strategy 3

3. Hadronic and Electromagnetic Energy Measurements with the DHCAL 6

3.1 Response of DHCAL to Hadrons 9

3.2 Response of DHCAL to Positrons 11

4. Summary 12

References 13

1. Introduction

After the successful construction and testing of the small size CALICE Digital Hadron Calorimeter (DHCAL) prototype, in the following named Vertical Slice Test (VST), with 20 cm x 20 cm Resistive Plate Chambers (RPCs), a larger prototype with 51 layers of 96 cm x 96 cm active area (1 cm x 1 cm pads) was built in 2008-2010. 38 layers were the DHCAL and 13 layers were the tail catcher section of the prototype. The performance characteristics of the RPCs and the readout system together with the results of the beam test data analysis of the VST with a maximum of 10 layers were encouraging towards the validation of the digital hadron calorimeter concept [1-6]. With this large size technical prototype, we observe hadron showers with unprecedented spatial resolution. Among the various physics and technical measurements the DHCAL offers, a first look at the data to investigate the hadronic and electromagnetic energy measurements with preliminary approaches is presented in this note. The details of the large size prototype is given in [7, 8].

2. Analysis Strategy

The data read out from the DHCAL contain the hit position information, the time stamp of the individual hits and the time stamp from the trigger and timing unit. Additionally, discriminated signals from a beam Čerenkov counter and a muon tagger are integrated into the data by the data acquisition system.

The hits in each layer are combined into clusters using a nearest-neighbor approach. If two hits share a common edge, they are assigned to the same cluster. The analysis presented in this note considers only the first 38 layers of the DHCAL and not the last 13 layers that were used as a tail catcher. The smallest layer number is the most upstream one. The event selection requires not more than 1 cluster in Layer 1 with at most four hits. This selection assures that upstream interactions are not included. The requirements of at least three active layers and no hits in the two outermost pads in any layer select the events with sufficient activity in the DHCAL and the events that have transverse containment, respectively.

The beam is a momentum selected mixture of muons, pions and positrons. This analysis is based on the topological particle identification utilizing the high segmentation of the DHCAL at beam momenta of 2, 4, 8, 12, 20, 25 and 32 GeV/c. Beam “momenta” and “energy” will be used interchangeably to refer to these numbers throughout this note.

The Muon identification is based on finding a linear alignment of isolated clusters within the DHCAL. The cluster in Layer 1 is matched with the clusters in the last layers and a line joining these clusters is formed. Then for all the layers in between, clusters with a distance less than 2 cm from the line are searched for. These clusters are required to be isolated from 1.5 cm to 25 cm from the predicted point. If the total number of layers with aligned clusters is equal to the total number of active layers (layers with at least one hit), the track is identified as a muon. An event display of such a muon is given in Fig. 1a. This case constitutes more than 60% of all the muons in a typical muon run. The remaining 40% of the muons have a few higher multiplicity

layers along the track which violate the isolation requirement. These high multiplicities are due to delta ray production and are not correlated between the layers. In order to tag these muon tracks, events with total number of layers with aligned clusters exceeding 80% of the number of active layers are considered. If the isolation criteria is not violated in two consecutive layers, the track is assigned a muon id. A muon track of this kind is displayed in Fig. 1b.

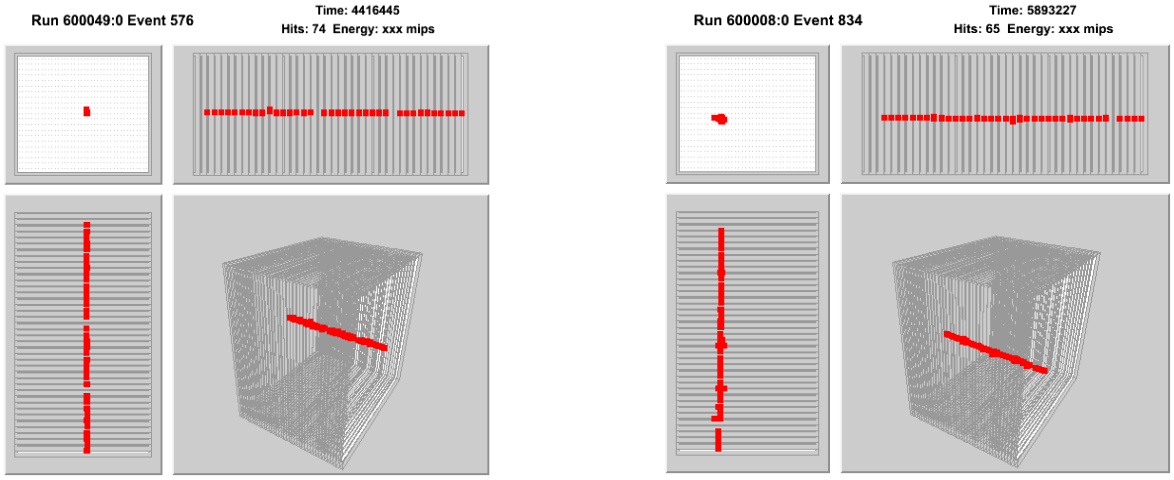

(a) **(b)**

Figure 1. Event display for a clean muon track (a) and a muon track with delta ray production in a few layers (b).

Figure 2 demonstrates the application of the muon identification algorithm to one of the muon runs. The algorithm is 97% efficient in identifying muons. The disagreement in the distributions is mainly in the higher end of the spectrum indicating that these muons have delta ray production in at least two consecutive layers or the tracks are highly inclined, hence the higher number of hits. 95% of the remaining, unidentified muons are excluded from the pion and positron analyses by requiring no hits in the last two layers of the DHCAL (longitudinal confinement requirement).

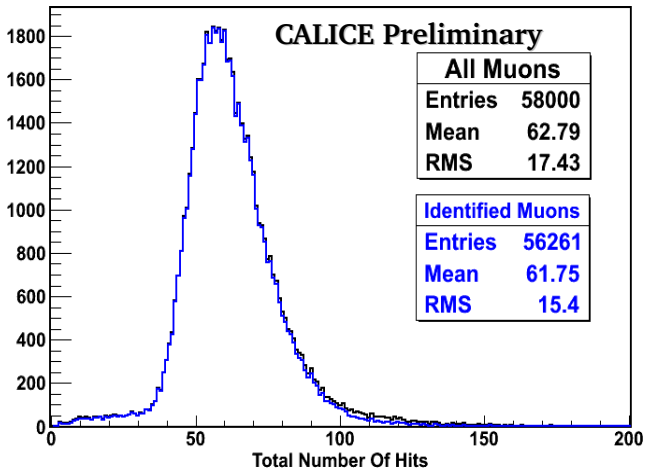

Figure 2. Distribution of the number of hits in muon data selected with the Muon-ID algorithm (blue histogram). The inclusive muon data is shown in black.

Once the muons are identified, the particle identification proceeds with finding the pions. First, the MIP segment is identified by a similar algorithm to the muon identification but this time looking for the alignment of clusters starting from the first layer and going towards the back of the calorimeter. Once the last MIP layer is determined (with having less than 4 hits), track segments from this layer towards the back of the DHCAL are searched for (track segment is defined as the aligned clusters in at least three layers). These track segments should not be aligned with the MIP segment. If any track segment that extends to at least four layers is found, the particle is identified as pion. For the track segments that extends only to three layers, the angle between these track segments is considered. If a pair with more than 20° angle in between is found, the particle is assigned a pion ID. These selections are based on the event topology in the interaction region of the pions. Event displays for a typical 4 GeV/c pion and positron are shown in Fig. 3a and 3b respectively. Figure 3a clearly depicts the MIP segment and the interaction region. The positron in Fig. 3b is not selected by the pion identification as there are no track segments satisfying the above requirements, and it is not identified as a muon due to the isolation requirement in muon identification.

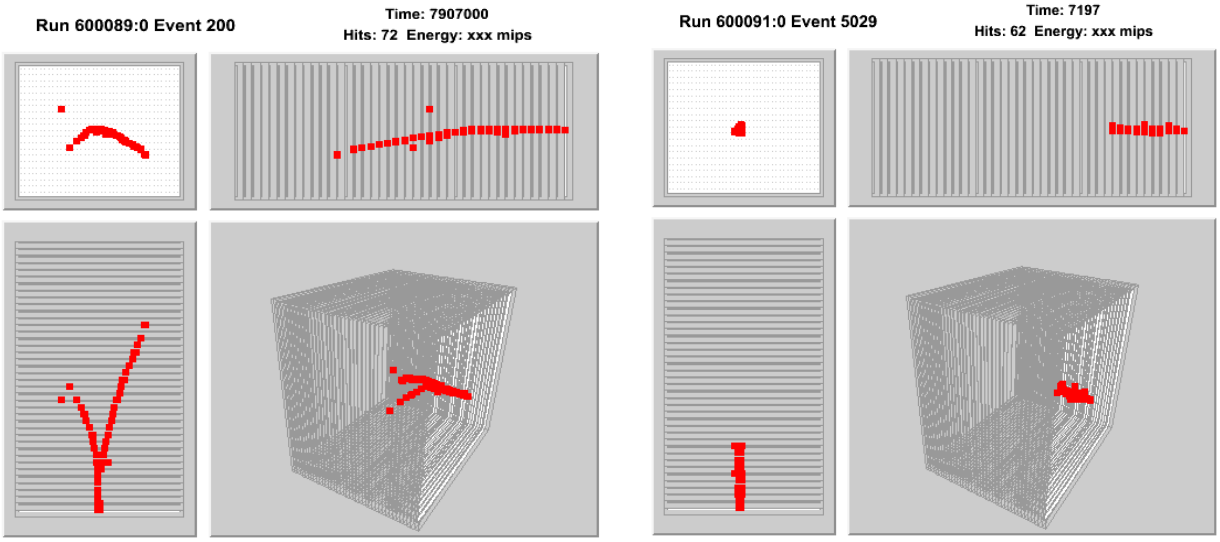

(a) (b)

Figure 3. A typical 4 GeV/c pion (a) and positron (b) event.

At the end of this step, the unidentified events contain all the positrons and a fraction of the pions. A transverse size parameter is defined to distinguish between the pions and the positrons in the remaining sample:

$$r_{rms} = \sqrt{\frac{\sum r_i^2}{N_{Hits}}}$$

where r_i is the distance of each hit to the x-y center of all the hits in the corresponding layer and N_{Hits} is the total number of hits. Figure 4 shows the distribution of the r_{rms} variable for the 20 GeV/c runs. A selection cut at $r_{rms}=5$ discriminates between the pions ($r_{rms}>5$) and positrons ($r_{rms}<5$) based on the differences between the transverse sizes of electromagnetic

and hadronic showers. The fraction of pions (positrons) identified by this cut is around 4% (100%) of all identified pions (positrons).

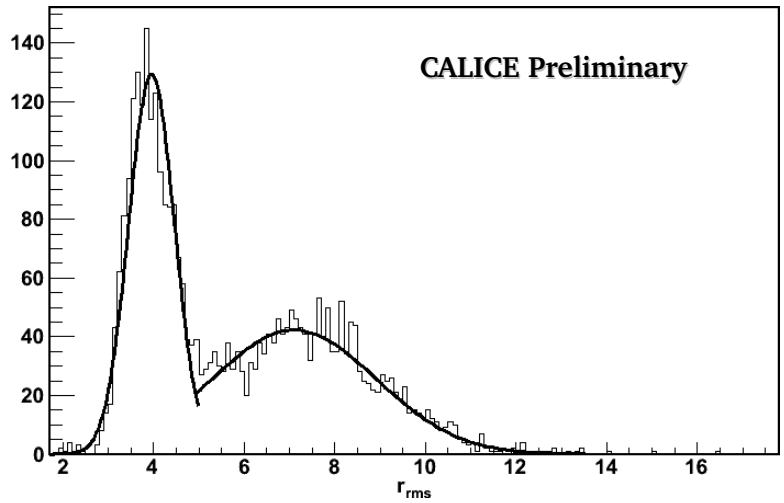

Figure 4. r_{rms} variable for the 20 GeV/c runs. Pions (positrons) tend to populate high (low) values of r_{rms}.

3. Hadronic and Electromagnetic Energy Measurements with the DHCAL

Below is a summary of the particle identification algorithms:

Muons: All active layers have aligned clusters with no more than two consecutive layers with non-isolated clusters.

Pions: At least one track segment in the interaction region that spans at least four layers. If such a track segment is not found, at least one pair of track segments that span three layers with at least 20° angle in between. These track segments should not be compatible with the beam (MIP segment) direction. If no track segment is found satisfying these requirements, $r_{rms} > 5$.

Positrons: $r_{rms} < 5$.

The overall event selection requires no more than one cluster in layer 1 with at most four hits, at least three layers with hits and no hits in the two outermost pads in any layer (transverse containment requirement). The longitudinal confinement requirement, which is used in the calorimetric measurements, further selects events with no hits in the last two layers of the DHCAL (layers 37 and 38).

Figures 5 a-n show the distribution of the total number of hits for pions and positrons after particle identification and longitudinal confinement requirement.

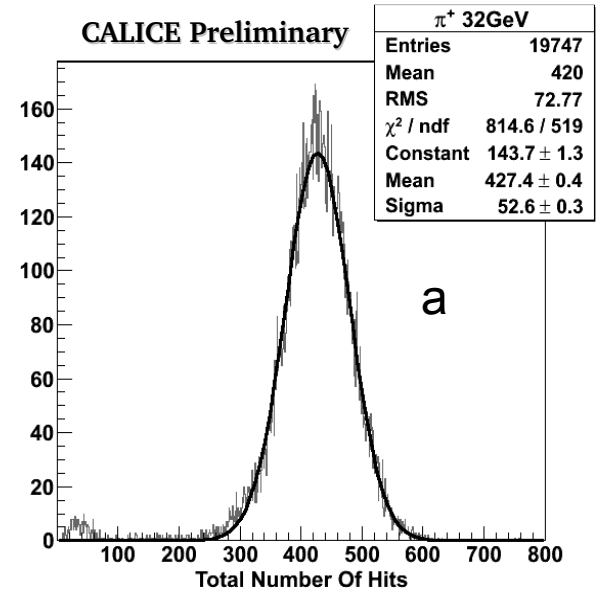
CALICE Preliminary
π+ 32GeV
Entries 19747
Mean 420
RMS 72.77
χ² / ndf 814.6 / 519
Constant 143.7 ± 1.3
Mean 427.4 ± 0.4
Sigma 52.6 ± 0.3
a
Total Number Of Hits

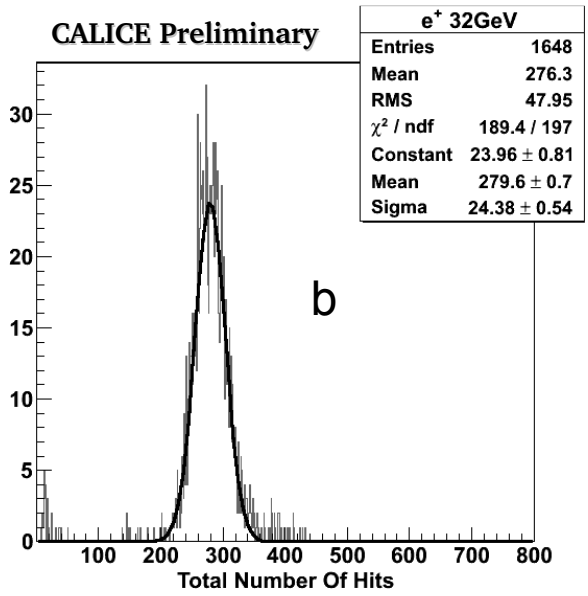
CALICE Preliminary
e+ 32GeV
Entries 1648
Mean 276.3
RMS 47.95
χ² / ndf 189.4 / 197
Constant 23.96 ± 0.81
Mean 279.6 ± 0.7
Sigma 24.38 ± 0.54
b
Total Number Of Hits

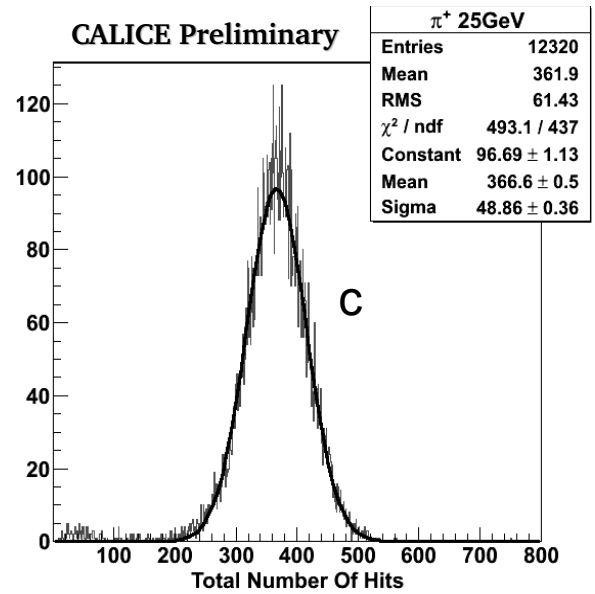
CALICE Preliminary
π+ 25GeV
Entries 12320
Mean 361.9
RMS 61.43
χ² / ndf 493.1 / 437
Constant 96.69 ± 1.13
Mean 366.6 ± 0.5
Sigma 48.86 ± 0.36
c
Total Number Of Hits

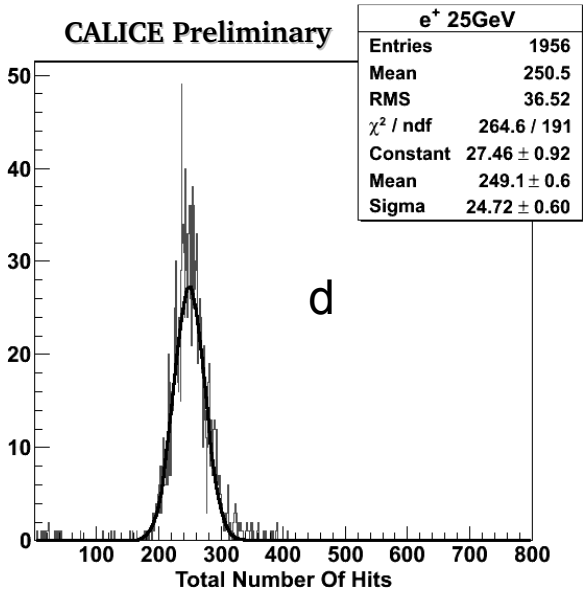
CALICE Preliminary
e+ 25GeV
Entries 1956
Mean 250.5
RMS 36.52
χ² / ndf 264.6 / 191
Constant 27.46 ± 0.92
Mean 249.1 ± 0.6
Sigma 24.72 ± 0.60
d
Total Number Of Hits

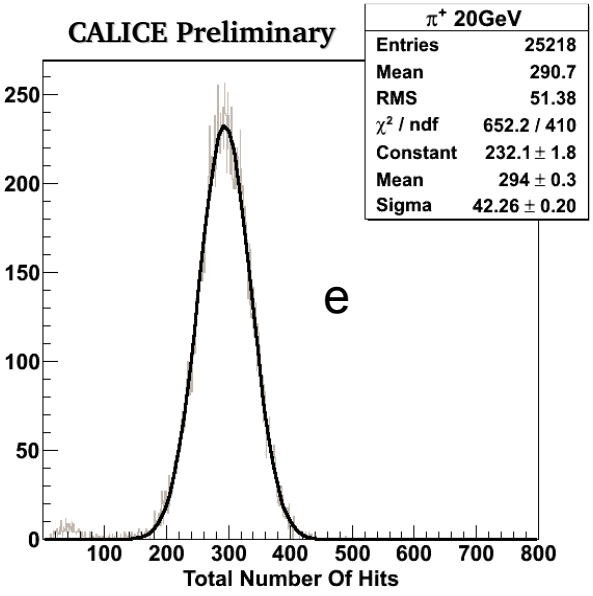
CALICE Preliminary
π+ 20GeV
Entries 25218
Mean 290.7
RMS 51.38
χ² / ndf 652.2 / 410
Constant 232.1 ± 1.8
Mean 294 ± 0.3
Sigma 42.26 ± 0.20
e
Total Number Of Hits

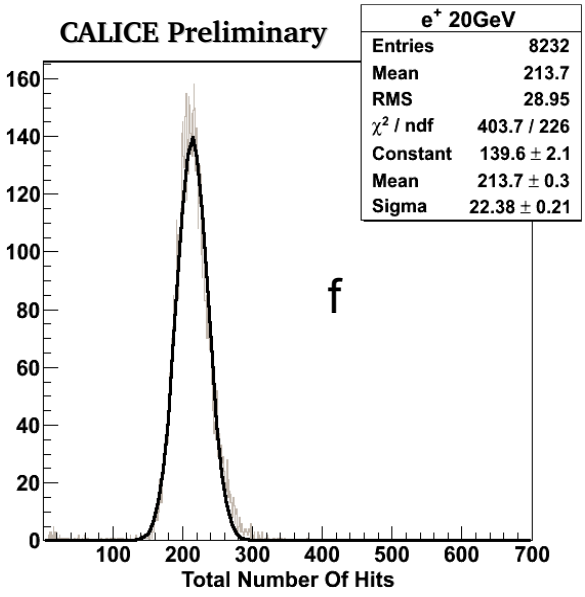
CALICE Preliminary
e+ 20GeV
Entries 8232
Mean 213.7
RMS 28.95
χ² / ndf 403.7 / 226
Constant 139.6 ± 2.1
Mean 213.7 ± 0.3
Sigma 22.38 ± 0.21
f
Total Number Of Hits

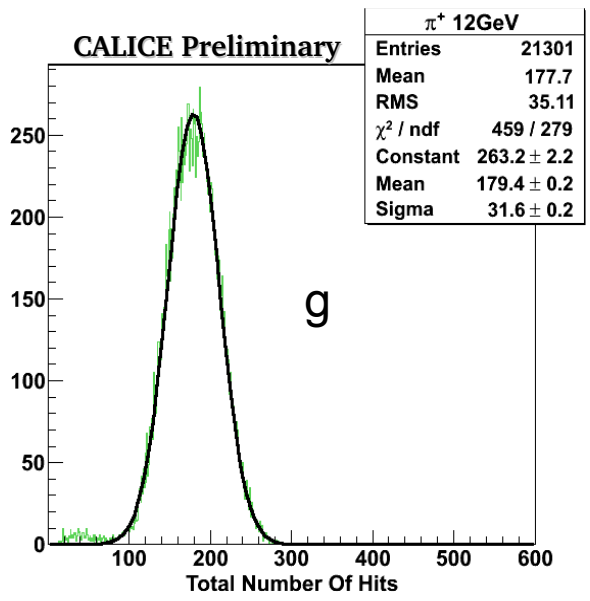
CALICE Preliminary
π+ 12GeV
Entries 21301
Mean 177.7
RMS 35.11
χ² / ndf 459 / 279
Constant 263.2 ± 2.2
Mean 179.4 ± 0.2
Sigma 31.6 ± 0.2
g
Total Number Of Hits

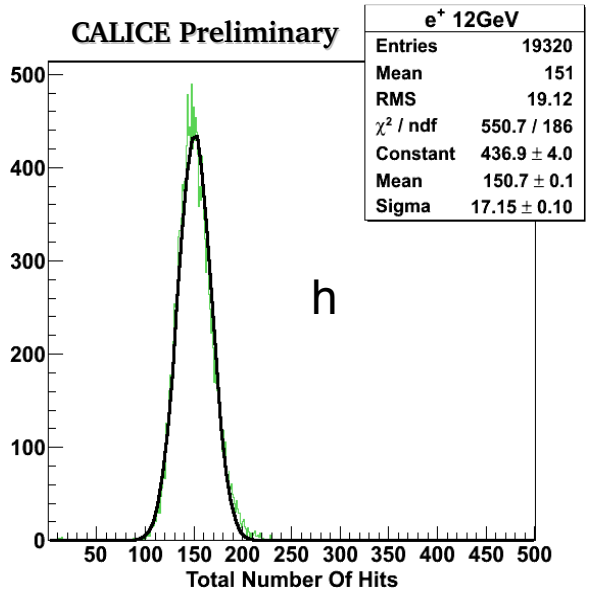
CALICE Preliminary
e+ 12GeV
Entries 19320
Mean 151
RMS 19.12
χ² / ndf 550.7 / 186
Constant 436.9 ± 4.0
Mean 150.7 ± 0.1
Sigma 17.15 ± 0.10
h
Total Number Of Hits

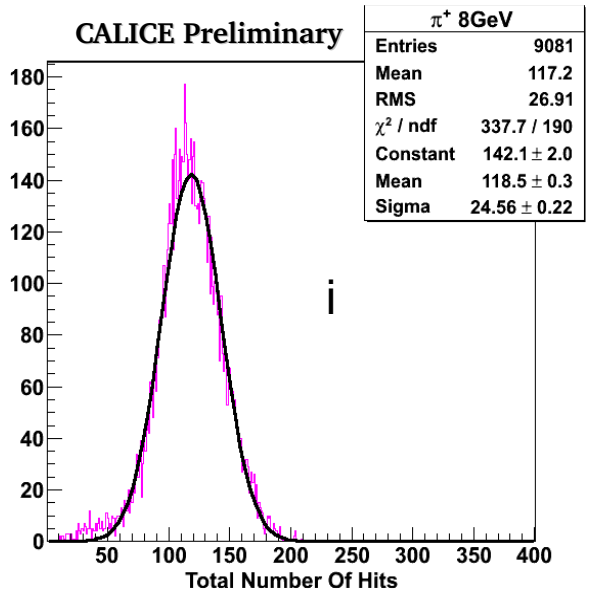
CALICE Preliminary
π+ 8GeV
Entries 9081
Mean 117.2
RMS 26.91
χ² / ndf 337.7 / 190
Constant 142.1 ± 2.0
Mean 118.5 ± 0.3
Sigma 24.56 ± 0.22
i
Total Number Of Hits

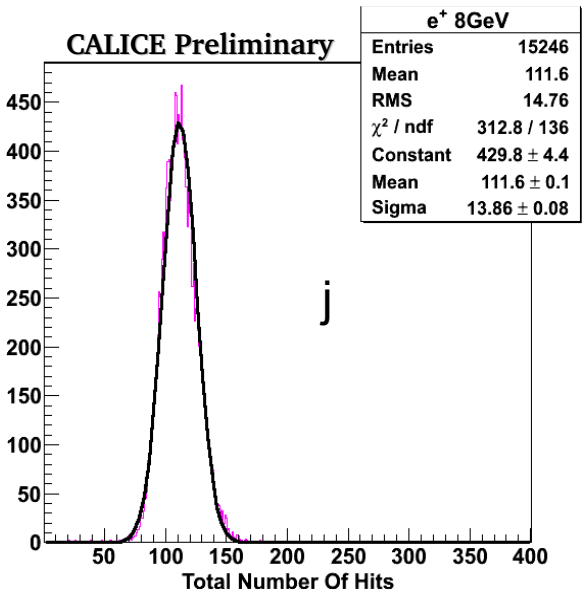
CALICE Preliminary
e+ 8GeV
Entries 15246
Mean 111.6
RMS 14.76
χ² / ndf 312.8 / 136
Constant 429.8 ± 4.4
Mean 111.6 ± 0.1
Sigma 13.86 ± 0.08
j
Total Number Of Hits

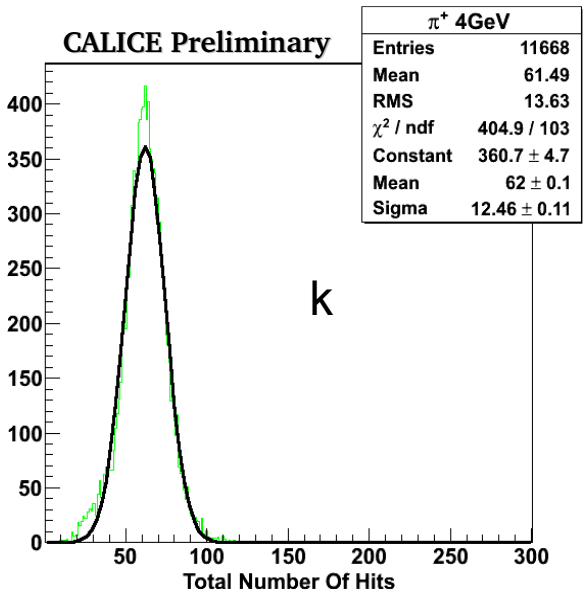
CALICE Preliminary
π+ 4GeV
Entries 11668
Mean 61.49
RMS 13.63
χ² / ndf 404.9 / 103
Constant 360.7 ± 4.7
Mean 62 ± 0.1
Sigma 12.46 ± 0.11
k
Total Number Of Hits

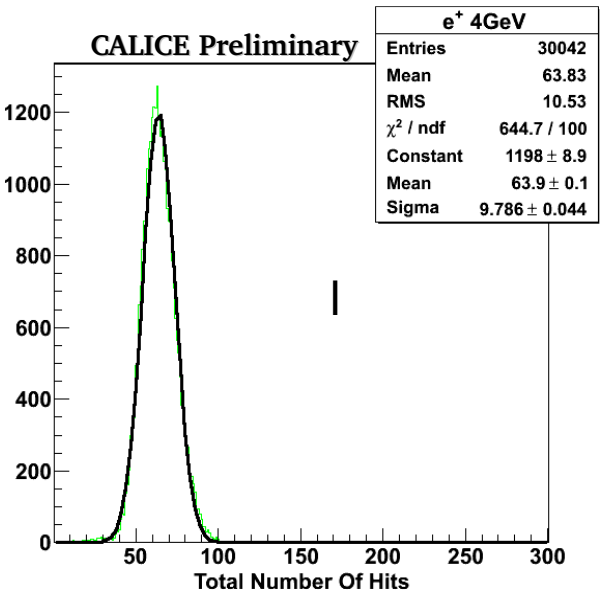
CALICE Preliminary
e+ 4GeV
Entries 30042
Mean 63.83
RMS 10.53
χ² / ndf 644.7 / 100
Constant 1198 ± 8.9
Mean 63.9 ± 0.1
Sigma 9.786 ± 0.044
l
Total Number Of Hits

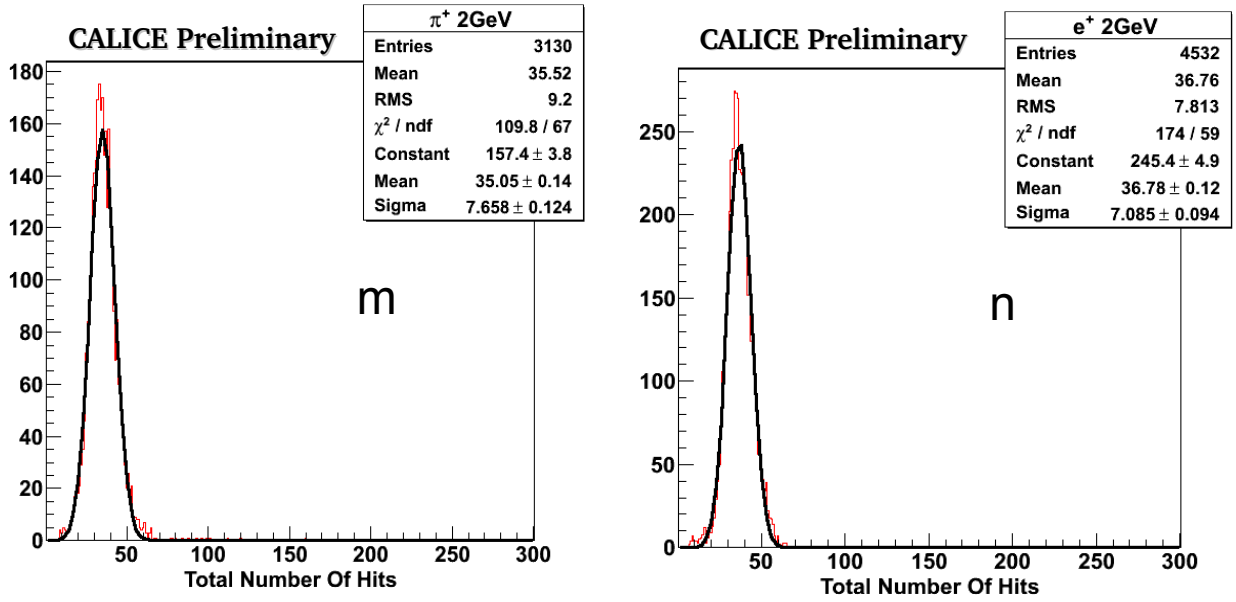

Figure 5. Distribution of total number of hits for 32, 25, 20, 12, 8, 4 and 2 GeV pions (a, c, e, g, i, k, m) and positrons (b, d, f, h, j, l, n) and the Gaussian fits.

At higher beam energies, the fraction of positrons in the beam is lower when compared to lower energies and the total hits spectra are well separated. At lower beam energies, the spectra overlap and the event topology has less discriminative power. Therefore the distributions in Figs. 5k, m are still significantly contaminated by positrons and unidentified low energy muons that have a higher probability of multiple scattering when compared to high energy ones. As additional tools and more sophisticated algorithms are being developed, 4 GeV and 2 GeV pion responses will be reported in future publications.

3.1 Response of DHCAL to Hadrons

The mean response of the DHCAL to pions is shown in Fig. 6a. Means, resolutions and the corresponding errors are determined from the Gaussian fits in Fig 5. The response is linear up to 25 GeV, and at 32 GeV the effect of saturation is evident. Therefore, 32 GeV data point is not included in the linear fit (N=aE where N is the total number of hits and E is the beam energy). Figure 6b shows the percent difference between measured and the fit values. Except the 32 GeV points, the deviation is within 2 %. Note that these results have been obtained without a calibration of the response of the DHCAL.

Figure 7 shows the hadronic energy resolution of the DHCAL with the current particle identification algorithms. 32 GeV points are excluded from the fits to the function

$$\frac{\sigma}{E}=\frac{\alpha}{\sqrt{E}}\oplus C$$

where α is the stochastic term and C is the constant term. The fits represent the data well and for the longitudinally contained pions -that have no hits in the last two layers- a stochastic term of approximately 55% and a constant term of 7.5% is achieved. The measurements are within 1-2% of predictions based on the simulation of the large-size DHCAL prototype using the VST results [2].

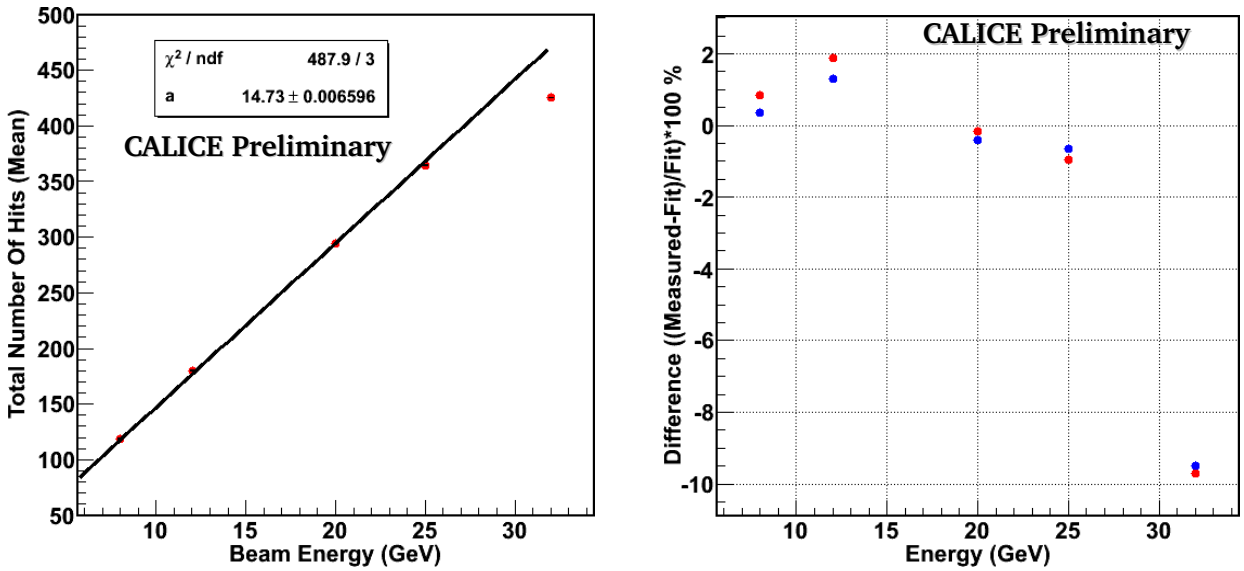

(a) (b)

Figure 6. The mean response of DHCAL to pions of 8, 12, 20, 25 and 32 GeV energy (a) and the difference between the measured and fit values for all identified pions (red) and longitudinally contained pions (no hits in the last two layers, blue) (b).

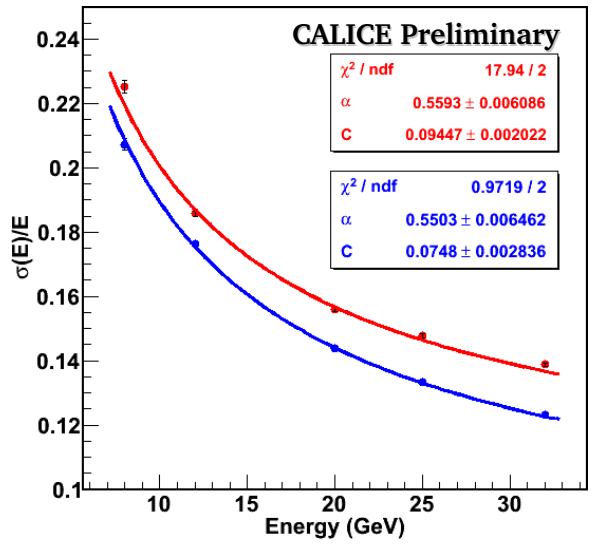

Figure 7. Hadronic energy resolution of DHCAL for all identified pions (red) and the longitudinally contained pions (blue).

3.2 Response of DHCAL to Positrons

The mean response of the DHCAL to identified positrons is shown in Fig. 8. The response is fit with the nonlinear function $N=a+bE^m$. The fit describes the data well and is in accordance with the predictions in the VST results of positron showers [4]. In order to measure the electromagnetic energy resolution of the DHCAL with the positron response corrected for non-linearity, the total number of hits for each positron event is mapped into its corresponding energy value using the fit function in Fig. 8. Then these reconstructed energy spectra are used to calculate the energy resolutions. Figure 9 shows the results of the energy reconstruction for 4 GeV (a) and 12 GeV (b) positron runs together with the Gaussian fits. Figure 10 shows the electromagnetic energy resolution for both uncorrected and corrected values.

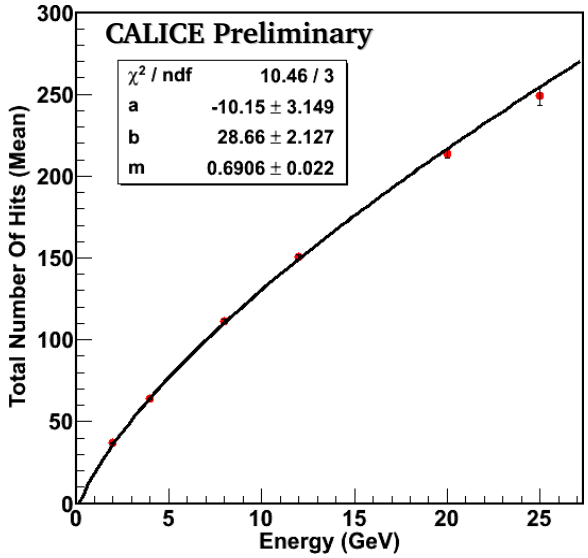

Figure 8. Mean response of DHCAL to positrons at 2, 4, 8, 12, 20 and 25 GeV.

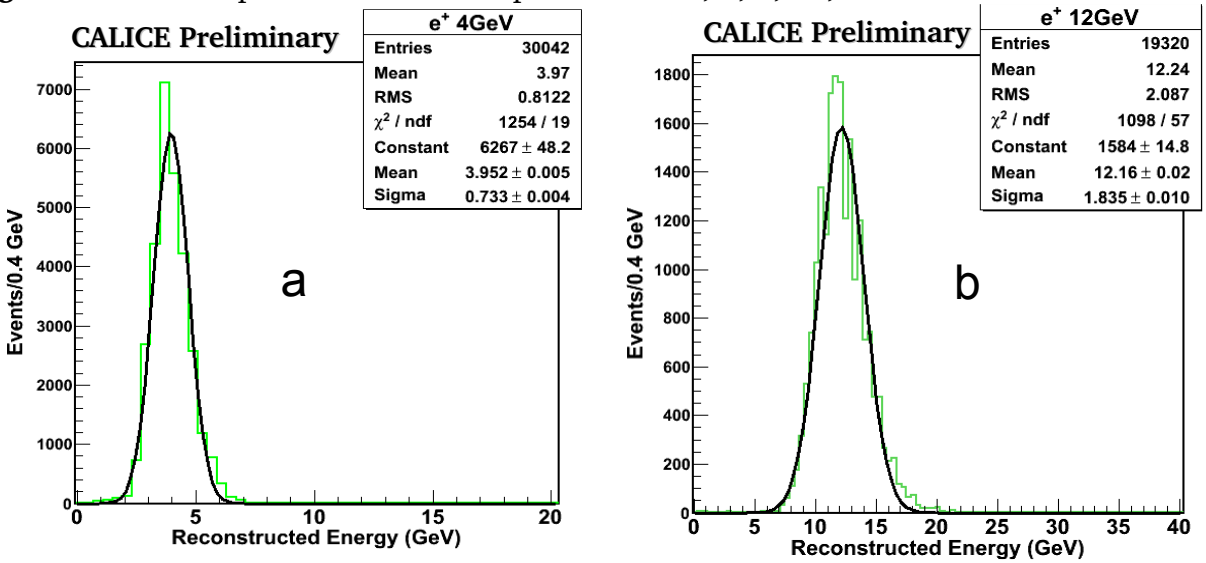

Figure 9. Reconstructed energy spectra for 4 GeV (a) and 12 GeV (b) positrons.

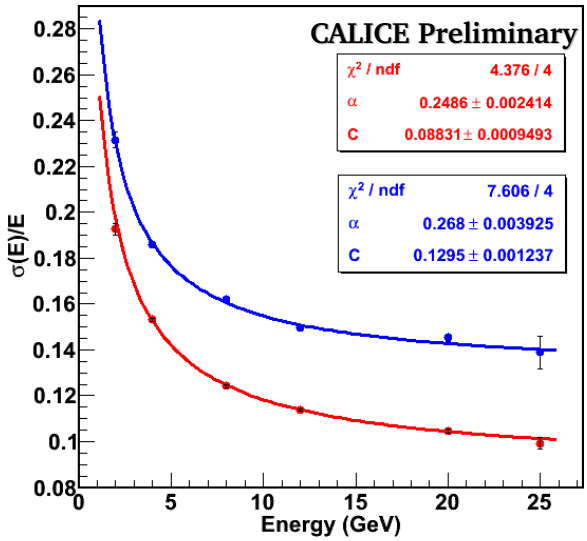

Figure 10. Corrected (blue) and uncorrected (red) electromagnetic energy resolution for DHCAL at 2, 4, 8, 12, 20 and 25 GeV.

4. Summary

With the two successful test beam campaigns in October 2010 and January 2011, the digital hadron calorimeter concept is being validated under extensive physics and technical tests. This note presents a first look analysis on the October 2010 data to obtain the digital hadron calorimeter properties. More sophisticated analyses will be forthcoming in the near future.

The particle identification algorithms defined within this text provide sufficiently well discrimination at high energies. However, the complications in the event topologies at low energies require further studies to integrate these energies into the calorimetric measurements. These new algorithms are expected to improve the current measurements as well. With the present algorithms, a hadronic energy resolution of $\frac{\sigma}{E}=\frac{55\%}{\sqrt{E}} \oplus 7.5\%$ and an electromagnetic energy resolution between 24% and 14% in the energy range of 2 – 25 GeV are obtained.

Further methods are being developed to obtain unbiased samples of pure beam particles and to obtain the DHCAL response not only as an energy measuring calorimeter, but also as a unique source of information of detailed hardonic interactions with unprecedented spatial resolution.

References

1. Q. Zhang et.al., “Environmental dependence of the performance of resistive plate chambers”, JINST 5 P02007, 2010.

2. B. Bilki et.al., “Hadron showers in a digital hadron calorimeter”, JINST 4 P10008, 2009.

3. B. Bilki et.al., “Measurement of the rate capability of Resistive Plate Chambers”, JINST 4 P06003, 2009.

4. B. Bilki et.al., “Measurement of positron showers with a digital hadron calorimeter”, JINST 4 P04006, 2009.

5. B. Bilki et.al., “Calibration of a digital hadron calorimeter with muons”, JINST 3 P05001, 2008.

6. G.Drake et al., Resistive Plate Chambers for hadron calorimetry: Tests with analog readout, Nucl. Instrum. Meth. A 578, 88, 2007.

7. http://www.hep.anl.gov/repond/DHCAL_FNAL_Nov_2010.pptx

8. CAN-030, “Analysis of DHCAL Muon Data”, 2011.